Bioorganic Chemistry 36 (2008) 121–127

Contents lists available at ScienceDirect

Bioorganic Chemistry

journal homepage: www.elsevier.com/locate/bioorg

Cloning, expression, purification, cofactor requirements, and steady state kinetics of phosphoketolase-2 from *Lactobacillus plantarum*

Alejandro Yevenes, Perry A. Frey *

Department of Biochemistry, University of Wisconsin–Madison, 1710 University Avenue, Madison, WI 53726, USA

ARTICLE INFO

Article history:
Received 19 November 2007
Available online 21 April 2008

Keywords:
Thiamine pyrophosphate
Phosphoketolase
Acetyl-thiamine pyrophosphate
Kinetics of phosphoketolase
Cloning phosphoketolase
Quaternary structure of phosphoketolase
Ordered equilibrium binding of metal-thiamine pyrophosphate to phosphoketolase
Ping pong kinetics of phosphoketolase

ABSTRACT

The genes *xpk1* and *xpk2*(*Δ1–21*) encoding phosphoketolase-1 and (Δ1–7)-truncated phosphoketolase-2 have been cloned from *Lactobacillus plantarum* and expressed in *Escherichia coli*. Both gene-products display phosphoketolase activity on fructose-6-phosphate in extracts. A N-terminal His-tag construct of *xpk2*(*Δ1–21*) was also expressed in *E. coli* and produced active His-tagged (Δ1–7)-truncated phosphoketolase-2 (hereafter phosphoketolase-2). Phosphoketolase-2 is activated by thiamine pyrophosphate (TPP) and the divalent metal ions Mg^{2+}, Mn^{2+}, or Ca^{2+}. Kinetic analysis and data from the literature indicate the activators are MgTPP, MnTPP, or CaTPP, and these species activate by an ordered equilibrium binding pathway, with Me^{2+}TPP binding first and then fructose-6-phosphate. Phosphoketolase-2 accepts either fructose-6-phosphate or xylulose-5-phosphate as substrates, together with inorganic phosphate, to produce acetyl phosphate and either erythrose-4-phosphate or glyceraldehyde-3-phosphate, respectively. Steady state kinetic analysis of acetyl phosphate formation with either substrate indicates a ping pong kinetic mechanism. Product inhibition patterns with erythrose-4-phosphate indicate that an intermediate in the ping pong mechanism is formed irreversibly. Background mechanistic information indicates that this intermediate is 2-acetyl-TPP. The irreversibility of 2-acetyl-TPP formation might explain the overall irreversibility of the reaction of phosphoketolase-2.

1. Introduction

Phosphoketolases play significant roles in energy metabolism by catalyzing the formation of acetyl phosphate (AcP)[1] and erythrose-4-phosphate (E4P) from fructose-6-phosphate (F6P), an intermediate in glycolysis, or of AcP and D-glyceraldehyde-3-phosphate (GAP) from xylulose-5-phosphate (Xu5P), an intermediate in the pentose phosphate pathway, according to Eqs. (1) and (2) [1]. AcP is a high energy molecule that can serve as a source of ATP by the action of

$$\text{F6P} + \text{P}_\text{i} \rightarrow \text{E4P} + \text{AcP} + \text{H}_2\text{O} \quad (1)$$

$$\text{Xu5P} + \text{P}_\text{i} \rightarrow \text{D-glyceraldehyde-3-P} + \text{AcP} + \text{H}_2\text{O} \quad (2)$$

acetate kinase or as a source of acetyl-CoA by the action of phosphotransacetylase. GAP produced from Xu5P by phosphoketolase is a glycolytic intermediate.

Phosphoketolases are key enzymes of the phosphoketolase pathway of obligatory and facultative heterofermentative lactic acid bacteria and the F6P shunt of bifidobacteria [2]. Classification of phosphoketolases follows substrate preferences, EC 4.1.2.9 when specificity is for Xu5P, and EC 4.2.1.22 when both Xu5P and F6P are accepted [3]. Phosphoketolase-2 from *Lactobacillus plantarum* is a fructose-6-phosphate phosphoketolase that accepts Xu5P and so is classified as EC 4.1.2.22.

Phosphoketolases are well known but little studied members of the family of thiamine pyrophosphate (TPP)-dependent enzymes. A limited literature on phosphoketolases describes activities in various microbial and eukaryotic sources, and limited information about molecular properties in several species is available [4–9].

Mechanistic information on the action of phosphoketolases is sparse, but the outlines of a general reaction mechanism appear to involve the transient formation of 2-(α,β-dihydroxyethylidene-TPP (DHETPP) and 2-acetyl-thiamine pyrophosphate (AcTPP) as intermediates [1,10–12]. As a TPP-dependent enzyme that presumably generates covalent substrate–TPP intermediates, the reaction of phosphoketolase can be expected to follow ping pong steady state kinetics, but no kinetic analysis is currently available.

* Corresponding author. Fax: +1 608 265 2904.
E-mail address: frey@biochem.wisc.edu (P.A. Frey).

[1] *Abbreviations used:* AcP, acetyl phosphate; AcTPP, 2-acetyl-thiamine pyrophosphate; ATP, adenosine 5′-triphosphate; DEAE, diethylaminoethyl; DHETPP, 2-(α,β-dihydroxyethylidene)-thiamine pyrophosphate; E4P, erythrose-4-phosphate; F6P, fructose-6-phosphate; GAP, glyceraldehyde-3-phosphate; HETPP, 2-hydroxyethylidene-thiamine pyrophosphate; IPTG, isopropyl-β-D-thiogalactoside; MES, 2-morpholinoethane sulfonic acid; MOPS, 3-(N-morpholino)propane sulfonic acid; NAD+, nicotinamide adenine dinucleotide; NADH, reduced NAD+; PMSF, phenylmethane sulfonylfluoride; Pi, phosphate ion; SDS–PAGE, sodium dodecylsulfonate–polyacrylamide gel electrophoresis; TPP, thiamine pyrophosphate.

0045-2068/$ - see front matter © 2008 Elsevier Inc. All rights reserved.
doi:10.1016/j.bioorg.2008.03.002

There is reason to expect at least one step in the hypothetical mechanism, the formation of AcTPP, to be irreversible. An irreversible step in a mechanism can be revealed by an unusual product inhibition profile. In this paper, we describe the cloning, expression, purification, and some molecular properties of (Δ1–7)-truncated phosphoketolase-2 from *L. plantarum*. We also describe the divalent metal ion preference, the kinetics for activation by divalent metal ions, and steady state kinetics in the action this enzyme.

2. Experimental

2.1. Materials

AcP, erythrose-4-phosphate, DEAE-Sepharose, F6P, 2-morpholinoethane sulfonic acid (MES), 3-(*N*-morpholino)propane sulfonic acid (MOPS), NAD^+, NADH, phenylmethane sulfonyl fluoride (PMSF), S-300 (Sephadex-300), streptomycin sulfate, TPP, and xylulose were purchased from Sigma Chemical Co. Other materials and suppliers were Ampicillin and Kanamycin, Fisher Biotech; Biogel P6, BioRad; isopropyl-β-D-thiogalactoside (IPTG, Promega; Ni–NTA, Qiagen; pET21a and pET28b(+), Novagen; tryptone and yeast extract, DIFCO. Xu5P was prepared by enzymatic phosphorylation of xylulose using xylulokinase and MgATP. The pNCO-xylB for overexpression of xylulokinase was kindly supplied by Professor A. Bacher and Dr. F. Rohdich of the Technische Universität München.

2.2. Assays

Relative protein concentrations were measured by the Bradford method using bovine serum albumin as the standard.

Initial rates of AcP formation were measured by the hydroxamate method [13]. In the standard assay, the reaction mixture consisted of 5 mM F6P, 1 mM TPP, 5 mM phosphate, 50 mM MES buffer at pH 6, and 5 mM $MgCl_2$ at 37 °C. The reaction was started by addition of phosphoketolase and stopped at timed intervals upon addition of 300 μL of 2 M hydroxylamine at pH 6.5, incubation 10 min at ambient temperature, and addition of 200 μL of 15% trichloroacetic acid, 200 μL of 4 M HCl, and 200 μL of 5% $FeCl_3$ in 0.1 M HCl. Samples were centrifuged at 21000*g* for 5 min, and the values of A_{505} of the supernatant fluids were measured.

In the ferricyanide reduction assay of phosphoketolase activity, the reaction mixtures consisted of 5 mM F6P, 50 mM MES buffer at pH 6, 1 mM TPP, 5 mM $MgCl_2$, and 1 mM ferricyanide at 37 °C. The reactions were started by addition of F6P and the rate of declining A_{420} measured; rates were calculated using the extinction coefficient 1000 M^{-1} cm^{-1} [14].

2.3. Cloning and expression in Escherichia coli of L. plantarum genes encoding phosphoketolase

Lactobacillus plantarum has two genes putatively encoding phosphoketolase, *xpk1* and *xpk2* [15]. The encoded amino acid sequences are 67% identical, and the amino acid sequence of XPK1 is 98% identical with that of the enzyme from *L. pentosus*. The two phosphoketolase genes from *L. plantarum* were cloned using PCR, the primers being designed to amplify the genomic regions1 to 2412 bp of gene *xpk1* encoding XPK1, and 22–2412 bp of *xpk2* encoding XPK2(Δ1–7), comprising the conserved domains predicted by sequence alignments [7,9,13].Truncation of *xpk2* deleted the N-terminal 7-amino acids, allowing the change of the starting codon UUG in the Lactobacillus genome to the first AUG as a starting codon, initiation being most efficient in *E. coli* with AUG. UUG is estimated to serve as initiator for only about 3% of the proteins in *E. coli* [16]. The two genes were amplified from genomic DNA (ATCC: BAA-793D™) by PCR and cloned in the expression vector pET21a(+) (Novagen). Amplification of *xpk1* employed the primers *xpk1*–1: 5′ TTA-AGA-ATT-CAA-CTG-CTT-ATT-TTA-AAC-CC 3′ (EcoRI site underlined) and *xpk1*–2: 5′ TTT-CAT-ATG-ACA-ACA-GAT-TAC-TCA-TCA-CC 3′ (NdeI site underlined). The PCR product was cloned into the expression vector pET21a(+) between the NdeI and EcoRI sites, yielding pET21a-*xpk1*. The recombinant plasmids were identified by agarose gel electrophoresis followed by DNA sequence analysis. Amplification of *xpk2* employed the primers *xpk2*–1: 5′ TGC-AAA-CAT-ATG-AGT-GAA-GCA-ATT-AAA-TCC 3′ (NdeI site underlined) and *xpk2*–2: 5′ GCT-GAG-CTC-TTG-ATT-AAA-ACT-CTA-CTT-CAA 3′ (SacI site underlined). The PCR product was cloned into the expression vector pET21a(+) between the NdeI and SacI sites, yielding pET21a-*xpk2*. The recombinant plasmids were identified as described pET21a-*xpk1*.

The recombinant plasmid, pET21a-*xpk1* or pET21a-*xpk2*, was transformed into *E. coli* BL21(DE3) and expression induced by IPTG at room temperature. The recombinant strains were grown in Luria–Bertani medium (10 g of tryptone per liter, 5 g of NaCl per liter, 5 g of yeast extract per liter) with 100 μg/mL of ampicillin at 37 °C to optical density of 0.3–0.5 and then induced with different concentrations of IPTG for 3 h at room temperature.

Both gene-products form inclusion bodies when expressed at 37 °C but are soluble when expressed at room temperature. Activities of phosphoketolases in cell extracts were maximal with 0.075 mM IPTG for phosphoketolase-1 and with 1 mM of IPTG for phosphoketolase-2, as determined by the ferricyanide reduction assay with F6P as the substrate.

The gene encoding phosphoketolase-2 from *L. plantarum*, excised from pET21a-*xpk2* by digestion with NdeI and SacI, was cloned into pET28b(+) between the NdeI and SacI sites. From the resultant construct pET28b-*xpk2*, phosphoketolase-2 was expressed with 6 histidine residues and recognition sites for thrombin in an N-terminal 20-amino acid histidine-tail. The recombinant plasmid pET28b-*xpk2* was transformed into *E. coli* BL21(DE3), and the recombinant strains were grown in Luria–Bertani medium (10 g of tryptone per liter, 5 g of NaCl per liter, 5 g of yeast extract per liter) with 50 μg/mL of kanamycin at 37 °C until A_{600} reached 0.3–0.5, and expression of phosphoketolase-2 was then induced with IPTG for 3 h at room temperature to produce soluble protein. Maximum activity in cell-free extracts was observed with 1 mM IPTG, similar to expression without the histidine-tail.

2.4. Purification of His-tagged phosphoketolase-2

The recombinant plasmid pET28b-*xpk2* was transformed into *E. coli* BL21(DE3), and the recombinant strains were grown in Luria–Bertani medium (10 g of tryptone per liter, 5 g of NaCl per liter, 5 g of yeast extract per liter) with 50 μg/mL of kanamycin at 37 °C to A_{600} of 0.3–0.5. Expression was then induced with 1 mM IPTG for 21 h at room temperature, and the cells were harvested by centrifugation. The cells (6.65 g from 2 L of culture) were resuspended in 7 mL of lysis buffer (50 mM MOPS pH 7.5; 200 mM NaCl; 0.2 mM PMSF), and sonicated four times for 15 s followed by 30 s on ice. The sonicate was centrifuged at 11,000*g* for 15 min at 4 °C. Streptomycin sulfate (2 mL of 30%) was added to the supernatant fluid and stirred at 4 °C for 15 min, and the mixture was centrifuged at 11,000*g* for 20 min at 4 °C. The supernatant fluid was dialyzed against 500 mL of lysis buffer for 6 h. Dialysis was repeated twice more with changes of buffer, first for 6 h and then for 12 h. The protein solution was then mixed with 5 mL of Ni–NTA resin (previously equilibrated in 50 mM MOPS pH 7.5; 200 mM NaCl) and incubated on ice for 30 min with occasional shaking. The mixture was centrifuged at 3000*g* and 4 °C and the resin washed with 3 volumes of 50 mM MOPS at pH 6, 3 volumes of

20 mM imidazole in 50 mM MOPS at pH 6, and 3 volumes of 50 mM imidazole in 50 mM MOPS at pH 6.

The protein was eluted with 4 volumes of 150 mM imidazole in 50 mM MOPS at pH 6. The resultant solution (20 mL) was loaded onto a column of Biogel P6 (1.5 × 47 cm), equilibrated and eluted with 50 mM MOPS at pH 7. This step was necessary because the protein lost activity in the presence of imidazole, a phenomenon that has been traced to complexation of the activating divalent metal cation by imidazole. The fractions containing phosphoketolase, as determined by the ferricyanide reduction assay and the assay for formation of AcP, were loaded on a column of Sephacryl-300 (2.5 × 46 cm), equilibrated and eluted in 50 mM MOPS at pH 7. The protein was obtained in ~90% of electrophoretic homogeneity in a yield of 58 mg (Table 1).

2.5. Purification of phosphoketolase-2 from L. plantarum

To purify phosphoketolase-2 without the histidine-tail, the recombinant strains with pET21a-*xpk2* were induced with 1 mM of IPTG for 21 h at room temperature. The cells (3.32 g from 1 L) were resuspended in 3 mL of lysis buffer (50 mM MOPS pH 7.0; 0.2 mM PMSF; 0.2 mM $MgCl_2$), and sonicated four times in bursts of 15 s followed by 30 s on ice. The mixture was centrifuged at 11,000*g* at 4 °C, and the supernatant fluid was loaded on a DEAE-Sepharose column (1.5 × 20 cm), previously equilibrated in 50 mM MOPS pH 7.0. The column was eluted with a 500 mL linear gradient increasing from 0 to 0.8 M NaCl in 50 mM MOPS at pH 7.0, and fractions containing phosphoketolase activity by the ferricyanide reduction assay were loaded on a Sephadex-300 column (2.5 × 46 cm), equilibrated and eluted in 50 mM MOPS pH 7. Phosphoketolase-2 was obtained in about 80% electrophoretic homogeneity in a yield of 28 mg (15% of the initial activity).

2.6. Steady state kinetics

Steady state kinetics methods were employed to determine the kinetic mechanisms for activation of phosphoketolase by complexes of TPP with divalent metal ions (Me^{2+}TPP) and for the kinetic mechanism in the action of phosphoketolase in the formation of AcP in the presence of saturating Ca^{2+}. In preliminary experiments, the initial rates of AcP formation were found to be constant and zero order for at least 30 min at pH 6.0 and 37 °C in MES buffer.

In studies of activation by Me^{2+}TPP, initial rates of AcP were measured varying the concentrations of F6P and the divalent metal ions. The assay mixtures contained 50 mM MES buffer at pH 6.0, 0.5 mM TPP, 15 mM phosphate (5 × K_m) and varying F6P and Me^{2+}. From the stability constants (K_{ST}) of MnTPP and MgTPP complexes [17] the concentrations of Me^{2+}TPP at each concentration of divalent metal ion could be calculated. The stability constant for CaTPP was not reported but was evaluated from a linear plot of six values of K_{ST} for various divalent metal ions [17] against the Me^{2+}-ionic radii. The value of K_{ST} for CaTPP was taken from the position of the ionic radius of Ca^{2+} in this plot. Double reciprocal plots of initial rates against [F6P] at several fixed [Me^{2+}TPP] were constructed.

The assay mixtures contained 50 mM MES buffer at pH 6.0, 0.5 mM TPP, 15 mM phosphate (5 × K_m) and varying F6P and Me^{2+}. Initial rates were determined in triplicate in activations by MnTPP and MgTPP and in duplicate for CaTPP. Eq. (3) for the equilibrium ordered binding mechanism and Eq. (4) for the equilibrium

$$v = VAB/(K_{ia}K_b + K_bA + AB) \quad (3)$$

$$v = VAB/(K_{ia}K_b + K_bA + K_aB + AB) \quad (4)$$

random binding mechanism were fitted to the data, where A = [Me^{2+}TPP] and B = [F6P]. In all cases Eq. (3) for the equilibrium ordered mechanism gave the best fit of data; fits of Eq. (4) gave very large values of error.

In the steady state kinetics of the phosphoketolase-catalyzed reaction of F6P or Xu5P with phosphate to give AcP, the initial rates of AcP were measured at varied concentrations of the sugar phosphate and phosphate. The assay mixtures contained 50 mM MES buffer at pH 6.0, 5 mM $CaCl_2$, 0.5 mM TPP and varying concentrations of P_i and either F6P or Xu5P. The reactions were started with 10 μg of His-tagged phosphoketolase-2, and each assay was repeated in triplicate. The rates of AcP formation were measured colorimetrically by the hydroxamate/$FeCl_3$ method. Eq. (4) for the sequential binding mechanisms and Eq. (5)

$$v = VAB/(K_bA + K_aB + AB) \quad (5)$$

for the ping pong mechanism were fitted to the initial rate data, where A and B were [sugar phosphate] and [P_i]. The best fits were to Eq. (5) for the ping pong mechanism.

In the product inhibition kinetics, the inhibiting product was E4P, and the varied substrates were F6P or P_i, respectively. Initial rates of AcP were measured by the hydroxamate/$FeCl_3$ method, with [F6P] as varied at several [E4P] and with [P_i] fixed at near half-saturation (3 mM). Initial rates were measured with [P_i] varied at several [E4P] and with [F6P] fixed at near half-saturation (25 mM). Eqs. (6)–(8) for competitive, noncompetitive, and uncompetitive inhibition were fitted to the data, where A represents concentration of the varied substrate, and I represents [E4P].

$$v = VA/K(1 + I/K_{is}) + A \quad \text{competitive} \quad (6)$$

$$v = VA/K(1 + I/K_{is}) + A(1 + I/K_{ii}) \quad \text{noncompetitive} \quad (7)$$

$$v = VA/K + A(1 + I/K_{ii}) \quad \text{uncompetitive} \quad (8)$$

3. Results

3.1. Purification and molecular properties of phosphoketolase-2

The genome of *L. plantarum* incorporates two genes annotated as phosphoketolases (*xpk*1 and *xpk*2 [15]. The encoded amino acid sequences are 67% identical. To study phosphoketolase from *L. plantarum*, both genes were cloned using PCR. Maximum activities for phosphoketolase-1 and phosphoketolase-2 in extracts were obtained by induction with 0.075 and 1 mM of IPTG, respectively. Both of the purified proteins catalyzed the TPP-dependent reduction of ferricyanide with F6P as the substrate, consistent with phosphoketolase activity. The purified proteins also catalyzed the production of AcP and E4P from F6P with TPP-dependence, verifying that they are phosphoketolases.

Table 1
Purification of histidine-tail phosphoketolase-2 from *L. plantarum*

Procedure	Activity[a] (U/mL)	Protein (mg/mL)	Specific activity (U/mg)	Volume (mL)	Total activity (U)	Total protein (mg)	Purification factor
Crude extract	2.81	54	0.052	7	20	378	1
Biogel P6	0.36	1.8	0.2	50	18	90	3.8
Sephacryl-300	1.22	2	0.61	29	34	58	11.7

[a] Activity was determined by the standard assay for formation of acetyl phosphate (see Section 2).

Heterologous expression in *E. coli* of *L. plantarum xpk2* from an expression vector incorporating a His-tag to the N-terminus (pET28b-*xpk2*), as described in Section 2 produces His-tagged phosphoketolase-2, and it is conveniently purified by use of a nickel chelating column (Table 1). Fig. 1 shows the analysis of the protein by SDS–PAGE from the cell-free extract through nickel-chelation and elution with imidazole. The band of phosphoketolase-2 migrates with an apparent molecular weight of 90 kDa, similar to the calculated subunit molecular weight based on the amino acid content.

The N-terminal His-tag does not appear to interfere with activity because the untagged phosphoketolase-2 produced by expression from the plasmid pET21a-*xpk2* and purified to about 70% homogeneity displayed activity comparable to that of the His-tagged enzyme.

3.2. Activation by divalent metal ions

Like other TPP-dependent enzymes, the activity of phosphoketolase-2 depends upon the presence of a divalent metal ion. The enzyme is not highly specific for divalent metals, although it might appear to be upon observation of relative activities and apparent K_m values with various divalent ions (appK_m^{Ca} = 160 μM, appK_m^{Mg} = 32 μM, appK_m^{Mn} = 0.4 μM). The apparent selectivity can be traced to the differential binding affinities of divalent metal ions to TPP. Values of stability constants (K_{ST}) for various Me^{2+}TPP complexes are available and range from 4.9×10^2 to 8.5×10^3 M^{-1} for the monocationic complexes, the dominant species at pH 6 [17]. Manganous ion has a much higher affinity for TPP ($K_{ST} = 3.6 \times 10^3$ M^{-1}) than Mg^{2+} ($K_{ST} = 6.6 \times 10^2$ M^{-1}), and Mn^{2+} activates phosphoketolase-2 at much lower concentrations than does Mg^{2+}. However, the maximum activities at saturating metal ions are comparable. The kinetics for reactions between divalent metal ions and TPP show very fast complexation, with equilibrium attained within milliseconds [17]. Therefore, in a typical assay of phosphoketolase-2, metal ion activation represents activation by a divalent metal complex, Me^{2+}TPP.

The kinetics of activation by MnTPP, MgTPP, and CaTPP, as evaluated by steady state analysis in which the concentrations of F6P and are varied at 15 mM P_i (~5K_m), indicate ordered equilibrium binding with Me^{2+}TPP leading. The kinetic parameters are given in Table 2, and the kinetic plots for activation by Ca, Mn, and MgTPP appear in Fig. 2. The best fits are of Eq. (3) for ordered equilibrium binding, with Me^{2+}TPP leading. When the data are plotted as reciprocal initial rates against [P_i] at several fixed [F6P], the lines

Table 2
Kinetic parameters for activation of phosphoketolase-2 by divalent metal complexes of TPP

Parameter[a]	CaTPP	MgTPP	MnTPP
V (IU mg prot^{-1})	1.0 ± 0.1	1.3 ± 0.1	1.0 ± 0.1
K_{ia} (μM)	115 ± 46	0.27 ± 0.07	24 ± 0.12
K_B (mM)	12 ± 4	21 ± 5	14 ± 6

[a] A =, B = F6P, V = maximum velocity, K_{ia} = dissociation constant for **E.**, and K_B = Michaelis constant for F6P.

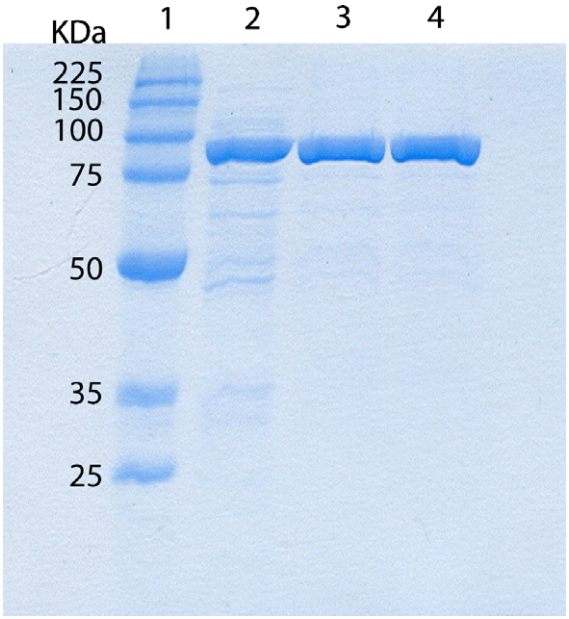

Fig. 1. Purification of His-tagged phosphoketolase-2 from *L. plantarum*. The SDS–PAGE analysis in lane 2 of cell-free extract of *E. coli* expressing the gene *xpk2* shows the overexpression of phosphoketolase-2. Lane 3 shows the SDS–PAGE analysis of His-tagged phosphoketolase-2 after purification by absorption to and elution from a nickel chelator, and lane 4 shows the protein after S-300 chromatography. The molecular weight markers are shown in lane 1.

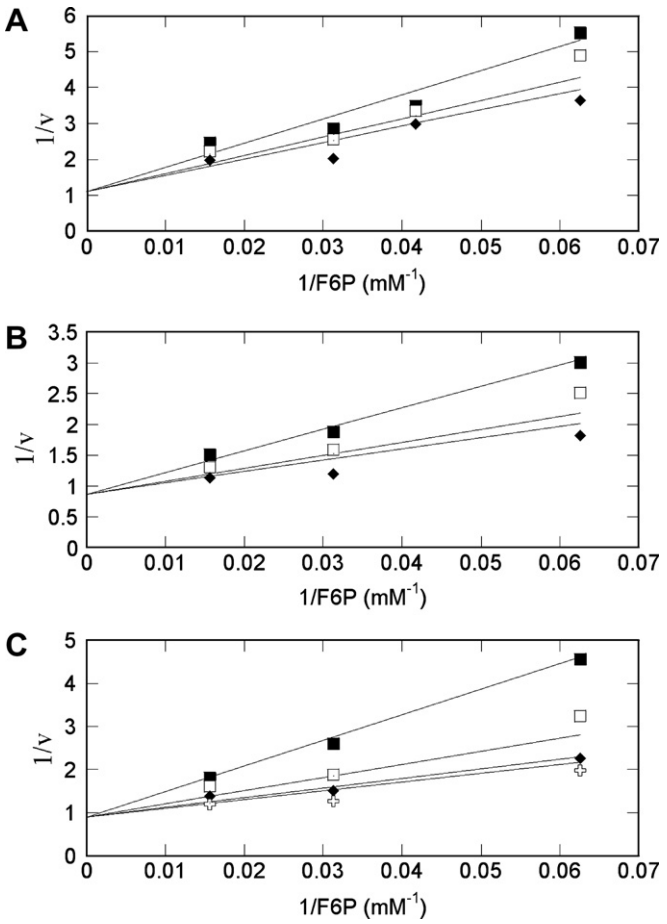

Fig. 2. Kinetic plots for activation of phosphoketolase-2 by divalent metal complexes of TPP. Shown are double reciprocal plots of initial rates for phosphoketolase-2 at pH 6.0 and 37 °C in 50 mM MES buffer. (A) Activation by MgTPP: the concentrations of F6P were 16, 24, 32, and 64 mM; and the concentrations of MgTPP were ■ 2.5 μM, □ 7.3 μM, and ♦ 18 μM. (B) Activation by MnTPP: the concentrations of F6P were 16, 24, 32, and 64 mM; and the concentrations of MnTPP were ■ 0.13 μM, □ 0.65 μM, and ♦ 3.2 μM. (C) Activation by CaTPP: the F6P concentrations of F6P were 8, 16, 32, and 64 mM; and the concentrations of CaTPP were ■ 27 μM, □ 90 μM, ♦ 250 μM, and ✣ 450 μM. The data in (A), (B), and (C) are fitted in Eq. (3) for equilibrium ordered binding, with binding first. The kinetic parameters for CaTPP, MgTPP, and MnTPP are given in Table 2.

converge at the left of the ordinate, in accord with Eq. (3). As shown in Table 2, the affinities of phosphoketolase-2 for MnTPP, MgTPP, and CaTPP are similar, though not identical, as are the maximum activities.

3.3. The steady state kinetic mechanism for reaction of phosphoketolase-2

The initial rates for the formation of AcP catalyzed by phosphoketolase-2 with F6P as the substrate are plotted in double reciprocal form in Fig. 3A and B. The data describe parallel lines, and Eq. (5), corresponding to a ping pong bi bi kinetic mechanism is fitted to the data. Xu5P as the substrate gives a similar pattern of parallel lines shown in Fig. 3C and D. Kinetic parameters for the reactions of F6P and Xu5P are included in Table 3.

Product inhibition by E4P is uncompetitive with respect to P_i and noncompetitive with respect to F6P, as illustrated in Fig. 4. This inhibition pattern is unusual for ping pong bi bi kinetic mechanisms. The first product to dissociate normally displays noncompetitive inhibition with respect to both substrates [18], as is found in the case of F6P as the varied substrate. With P_i as the varied substrate, uncompetitive inhibition by E4P must be explained. The rationale for the uncompetitive pattern in Fig. 4 is given in Section 4 in connection with a minimal kinetic mechanism.

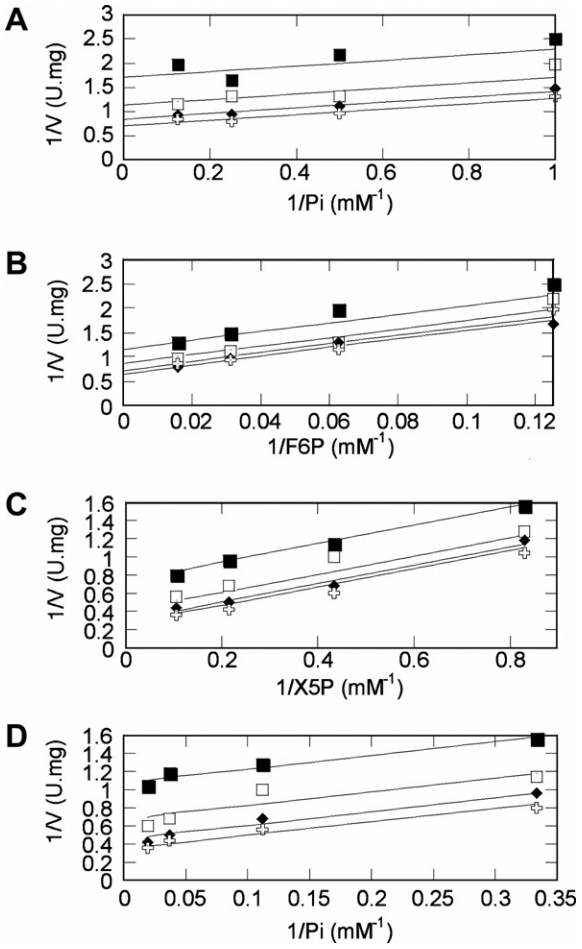

Fig. 3. Kinetic plots of initial rates for the overall reaction of phosphoketolase-2. (A–D) Double reciprocal plots of initial rates AcP formation in the reactions of F6P or Xu5P with P_i. (A) The varied concentrations of P_i were 1, 2, 4, and 8 mM, and the changing fixed concentrations of F6P were ■ 8 mM, □ 16 mM, ♦ 32 mM, and ✣ 64 mM. (B) The varied concentrations of F6P were 8, 16, 32, and 64 mM; and the changing fixed concentrations of P_i were ■ 1 mM, □ 2 mM, ♦ 4 mM, and ✣ 8 mM. (C) The varied concentrations of Xu5P were 1.2, 2.3, 4.6, and 9.3 mM; and the changing fixed concentrations of P_i were ■ 3 mM, □ 9 mM, ♦ 27 mM, and ✣ 54 mM. (D) The varied concentrations of P_i were 3, 9, 27, and 54 mM, and the changing fixed concentrations of Xu5P were ■ 1.2, □ 2.3, ♦ 4.6, and ✣ 9.3 mM. The parallel lines are fitted in Eq. (5) for the ping pong bi bi kinetic mechanism, and he kinetic parameters are given in Table 3.

Table 3
Kinetic parameters for reactions of F6P or Xu5P with P_0 in the reaction of phosphoketolase-2

Substrates	F6P and Pi	Xu5P and Pi
k_{cat} [E] = V (IU mg^{-1})	1.8 ± 0.2	4.1 ± 0.4
K_a (mM)[a]	24 ± 4	3.6 ± 0.6
K_b (mM)[a]	2.9 ± 0.5	7.5 ± 1.3
K_{is}^{E4P} (mM)	8 ± 4	nd[b]
K_{ii}^{E4P} (mM)	4.4 ± 0.9	nd[b]

[a] K_a, Michaelis constant for F6P (K_m^{F6P} in Eqs. (9) and (10)) or Xu5P; K_b, Michaelis constant for P_i (K_m^{P} in Eqs. (9) and (10)).
[b] Not determined.

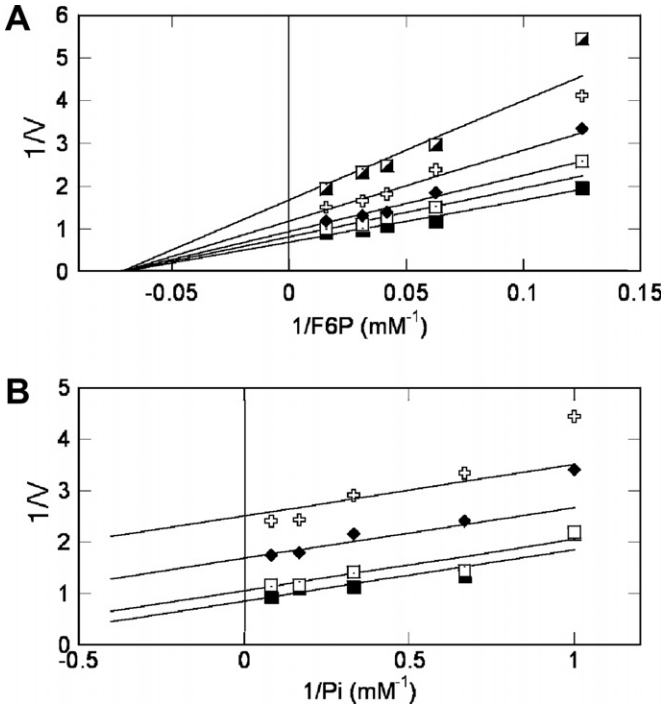

Fig. 4. Product inhibition of phosphoketolase-2 by E4P. The reaction mixtures contained 50 mM MES at pH 6, 5 mM $CaCl_2$, and 0.5 mM TPP together with varied concentrations of F6P, P_i, and E4P. (A) F6P varied: the concentrations of F6P were 8, 16, 24, 32, and 48 mM; and the constant substrate (phosphate) was 3 mM. The concentrations of E4P were ◪ 8 mM, ✣ 4 mM, ♦ 2 mM, □ 1 mM, and ■ 0 mM. (B) P_i varied: the concentrations of the variable substrate (P_i) were 1, 1.5, 3, 6, and 12 - mM; and the constant substrate (F6P) was 25 mM. The concentrations of erythrose-4-phosphate (E4P) were ✣ 8 mM, ♦ 4 mM, □ 1 mM, and ■ 0 mM.

4. Discussion

4.1. Kinetics in the action of phosphoketolase-2

Scheme 1 shows the simplest and most likely ping pong kinetic mechanism for the overall action of phosphoketolase-2 on F6P, where TPP refers to Me^{2+}TPP and Me = Ca^{2+}, Mg^{2+}, or Mn^{2+}.

The rate constants are numbered following the convention that forward constants are odd-numbered and reverse constants are even-numbered. In the absence of E4P, k[E4P] = 0, and the initial rate law is Eq. (9), the same form as Eq. (5),

$$v = \frac{k_{cat}[E][F6P][P_i]}{[F6P][P_i] + K_m^{F6P}[P_i] + K_m^{P}[F6P]} \quad (9)$$

where $k_{cat} = k_3k_5k_9/(k_5k_9 + k_3k_9 + k_3k_5)$, $K_m^{F6P} = [k_5k_9(k_2 + k_3)]/[k_1(k_5k_9 + k_3k_9 + k_3k_5)]$, and $K_m^{P} = [k_3k_5(k_8 + k_9)]/[k_7(k_5k_9 + k_3k_9 + k_3k_5)]$. In Eq. (5), $K_b = K_m^{F6P}$ and $K_a = K_m^{P}$. In the ping pong mechanism, **E.**DHETPP and **E.**AcTPP are intermediates generated in the reaction of F6P with **E.**TPP independently of the second substrate P_i. According to the mechanism, F6P reacts with the complex of phosphoketolase-2 and to form enzyme-bound DHETPP and release E4P in the absence of P_i. DHETPP undergoes dehydration irreversibly at the active site to AcTPP, and P_i then binds to the enzyme, accepts the acetyl group from AcTPP, and AcP undergoes dissociation.

Irreversibility in the dehydration of DHETPP to AcTPP explains uncompetitive inhibition by E4P with respect to P_i. By Cleland's Rules [18], E4P and P_i bind to different forms of the enzyme, **E.**DHETPP and **E.**AcTPP, respectively, giving an intercept effect in the double reciprocal plots with varying [P_i]. Because of irreversibility in the dehydration of **E.**DHETPP, no reversible step connects these two enzyme forms, so there is no slope effect, and the inhibition is uncompetitive. The product inhibition reveals a special case of the ping pong bi bi mechanism, wherein an irreversible step makes one inhibition pattern uncompetitive instead of the usual noncompetitive pattern observed when all steps are reversible. Noncompetitive inhibition by E4P with respect to F6P arises from the binding of E4P and F6P to different enzyme forms **E.**DHETPP and **E.**TPP, which are connected by reversible steps.

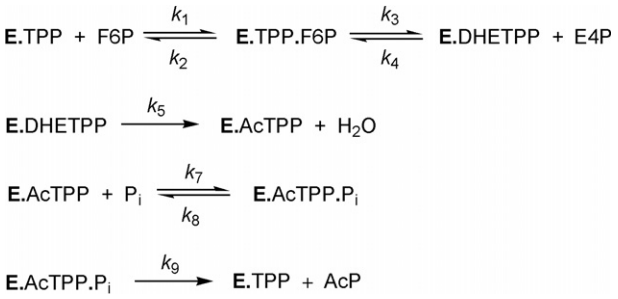

Scheme 1. A kinetic mechanism for phosphoketolase-2.

Accordingly, Eq. (10) is the initial rate law for the mechanism in Scheme 1 when E4P is present and product inhibition occurs

$$v = \frac{k_{cat}[E][F6P][P_i]}{[F6P][P_i] + K_m^{F6P}[P_i]\left(1 + \frac{[E4P]}{K_{is}^{E4P}}\right) + K_m^{P}[F6P]\left(1 + \frac{[E4P][P_i]}{K_{ii}^{E4P}}\right)} \quad (10)$$

In Eq. (10), k_{cat}, K_m^{F6P}, and K_m^{P} are as in Eq. (9), and $K_{is} = [k_5(k_2 + k_3)]/k_2k_4$ and $K_{ii} = [k_3k_5(k_8 + k_9)]/k_4k_7k_9$. Eq. (10) takes the form of noncompetitive inhibition by E4P, when F6P is the varied substrate, and uncompetitive inhibition when P_i is the varied substrate, in accord with Fig. 4. Values for K_{is} and K_{ii} are given in Table 3.

The kinetic mechanism in Scheme 1 predicts that phosphoketolase catalyzes the exchange of E4P with F6P in the absence of P_i. The literature is confused on this point. In one study, no corresponding exchange of [^{14}C]GAP/Xu5P could be observed [4] whereas in another study DHETPP could be transformed with GAP into Xu5P [1,19]. In the earlier study, the concentration of [^{14}C]GAP was quoted as "trace", implying unknown and very low. A low concentration of GAP would not react rapidly and could lead to a false negative result. The product inhibition constants in this report support the kinetic mechanism in Scheme 1 and the results of the transformation of DHETPP and GAP into Xu5P, as reported [1,19].

Phosphoketolase from *L. plantarum* does not catalyze any reversal of the formation of AcTPP, even enolization to enolacetyl-TPP,

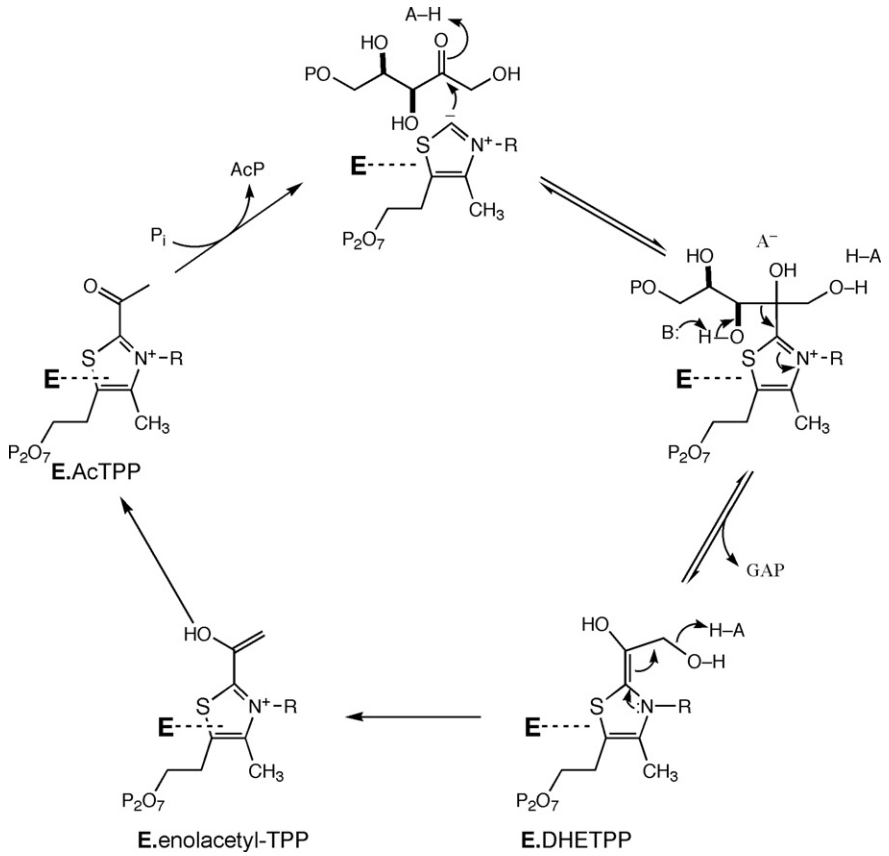

Scheme 2. A chemical mechanism for phosphoketolase-2.

because a study in [^{3}H]H_2O with arsenate as the acceptor led to one equivalent of tritium in acetate. Based on this result, Goldberg and Racker wrote: "This indicates that the formation of acetate does not involve labialization of the hydrogen atoms on the β-carbon of the thiamine-linked intermediate" [20], the intermediate being DHETPP. Furthermore, phosphoketolase does not catalyze an exchange of $^{32}P_i$ with AcP, showing that the reaction of P_i with AcTPP at the active site is irreversible as well.

All things considered, available information from the literature and this paper support the mechanism in Scheme 2 for the action of phosphoketolase on Xu5P. In this mechanism, AcTPP arises from dehydration of the initial adduct between the substrate and TPP, followed by ketonization of the resultant enolacetyl-TPP. Both dehydration and ketonization appear to be irreversible processes. This mode of AcTPP formation differs from the oxidative processes leading to AcTPP in the reactions of TPP-dependent oxidases and oxidoreductases, in which electron transfer from 2-hydroxyethylidene-TPP (HETPP) leads to AcTPP [21–24].

The dehydration of DHETPP in Scheme 2 is analogous to the mechanism by which 3-fluropyruvate generates AcTPP in the active site of pyruvate dehydrogenase, component E1 in the pyruvate dehydrogenase complex [25,26]. Pyruvate dehydrogenase accepts 3-fluorpyruvate as a substrate and catalyzes its decarboxylation and defluorination in the presence of dihydrolipoate to form *S*-acetyldihydrolipoate. The mechanism follows that for the decarboxylation of pyruvate to form β-fluoro-α-hydroxyethylidene-TPP, which undergoes elimination of fluoride to generate 2-enolacetyl-TPP, analogous to the dehydration of DHETPP in Scheme 2. Ketonization of 2-enolacetyl-TPP to AcTPP and acetyl group transfer to dihydrolipoate produces *S*-acetyldihydrolipoate, a step analogous to the reaction of phosphate with AcTPP in Scheme 2.

Acknowledgment

This research was supported by Grant GM30480 from the National Institute of General Medical Sciences.

References

[1] L.O. Krampitz, Annu. Rev. Biochem. 38 (1969) 213–240.
[2] B. Pieterse, R.J. Leer, H.J. Schurem, M.J. van der Werf, Microbiology 151 (2005) 3881–3894.
[3] A. Bairoch, Nucleic Acids Res. 28 (2000) 304–305.
[4] E.C. Heath, J. Hurwitz, B.L. Horecker, A. Ginsburg, J. Biol. Chem. 231 (1958) 1009–1029.
[5] J.P. Grill, J. Crociani, J. Ballongue, Curr. Microbiol. 31 (1995) 49–54.
[6] K.G. Fandi, H.M. Ghazali, A.M. Yazid, A.R. Raha, Lett. Appl. Microbiol. 32 (2001) 235–239.
[7] J.M. Lee, D.W. Jeong, O.K. Koo, M.J. Kim, J.H. Lee, H.C. Chang, J.H. Kim, H.J. Lee, Biotechnol. Lett. 27 (2005) 853–858 (Erratum in: Biotechnol Lett. 27 (16) 1247).
[8] C. Ingram-Smith, S.R. Martin, K.S. Smith, Trends Microbiol. 14 (2006) 249–253.
[9] C.C. Posthuma, R. Bader, R. Engelmann, P.W. Postma, W. Hengstenberg, P.H. Pouwels, Appl. Environ. Microbiol. 68 (2002) 831–837.
[10] P.A. Frey, Biofactors 2 (2002) 1–9.
[11] I. Merkler, J. Retey, Eur. J. Biochem. 120 (2002) 593–597.
[12] W. Schöter, H. Holzer, Biochim. Biophys. Acta 77 (1963) 474–484.
[13] L. Meile, L.M. Rohr, T.A. Geissmann, M. Herensperger, M. Teuber, J. Bacteriol. 183 (2001) 2929–2936.
[14] G.A. Kochetov, Methods Enzymol. 89 (1982) 43–44.
[15] M. Kleerebezem, J. Boekhorst, R. van Kranenburg, D. Molenaar, O.P. Kuipers, R. Leer, R. Tarchini, S.A. Peters, H.M. Sandbrink, M.W. Fiers, W. Steikema, R.M. Lankhorst, P.A. Bron, S.M. Hoffer, M.N. Groot, R. Kerkhoven, M. de Vries, B. Ursing, W.M. de Vos, R.J. Siezen, Proc. Natl. Acad. Sci. USA 100 (2003) 1990–1995.
[16] F.R. Blattner, G. Plunckett 3rd, C.A. Bloch, N.T. Perna, V. Burland, M. Riley, J. Collado-Vides, J.D. Glasner, C.K. Rode, G.F. Mayhew, J. Gregor, N.W. Davis, H.A. Kirkpatrick, M.A. Goeden, D.J. Rose, B. Mau, Y. Shao, Science 277 (1997) 1453–1474.
[17] H.B. Katz, K. Kustin, Biochim. Biophys. Acta 313 (1973) 235–248.
[18] W.W. Cleland, The Enzymes, third ed., vol. 2, pp. 1–65.
[19] R. Votaw, W.T. Williamson, L.O. Krampitz, W.A. Wood, Biochem. Z. 338 (1963) 756–762.
[20] M.L. Goldberg, E. Racker, J. Biol. Chem. 237 (1962) 3841–3842.
[21] K.J. Gruys, A. Atta, P.A. Frey, Biochemistry 28 (1989) 9071–9080.
[22] K. Tittmann, G. Wille, R. Golbik, A. Weidner, S. Ghisla, G. Hübner, Biochemistry 44 (2005) 13291–13303.
[23] K. Tittmann, R. Golbik, S. Ghisla, G. Hübner, Biochemistry 39 (2000) 10747–10754.
[24] G. Wille, D. Meyer, A. Steinmetz, E. Hinze, R. Golbik, K. Tittmann, Nat. Chem. Biol. 2 (2006) 324–328.
[25] L.S. Leung, P.A. Frey, Biochem. Biophys. Res. Commun. 81 (1978) 274–279.
[26] D.S. Flournoy, P.A. Frey, Biochemistry 25 (1986) 6036–6043.